Joakim Sundnes,[*] Andrew D. McCulloch[†]

Computational heart mechanics

Apr 24, 2019

Springer

[*] Simula Research Laboratory and Department of Informatics, University of Oslo.
[†] Bioengineering Department, University of California, San Diego.

Preface

The purpose of this book is to introduce students and researchers to the principles of computational soft tissue mechanics, and provide them with the necessary background to use, understand and potentially build computational software for heart mechanics. A brief general introduction to nonlinear solid mechanics is given, but the reader is referred to other books for a more detailed explanation of these topics. Obtaining one of these books is highly recommended, since the present tex is compact and may be difficult to read without any background in continuum mechanics. The book will include a number of relevant examples that give the reader both an idea of what the models can be used for, and a collection of "recipes" for using and solving the models.

From the doconce book setup:

1. Chapters can exist as stand-alone documents in different formats:
   - traditional LaTeX-style PDF report,
   - web pages with various fancy stylings (e.g., Sphinx, Bootstrap) and possibility for multi-media elements,
   - IPython notebooks,
   - blog posts (not exemplified here, but straightforward[1]),
   - wiki (if you do not need mathematical typesetting).
2. Chapters can be flexibly assembled into a traditional LaTeX-based PDF book for a traditional publisher, or a fancy ebook.
3. The book and the individual chapter documents may have different layouts.
4. Active use of preprocessors (Preprocess and Mako) makes it easy to have different versions of the chapters, e.g., a specialized version for a course and a general version for the world book market).

[1] `http://hplgit.github.io/doconce/doc/pub/manual/html/manual.html#blog-posts`

5. DocOnce has support for important elements in teaching material: eye-catching boxes (admonitions), quizzes, interactive code, videos, structured exercises, quotes.
6. Study guides or slides can easily be developed from the running text and stored along with the chapters. These can be published as LaTeX Beamer slides, reveal.js slides, and IPython notebooks.

These features have the great advantage that a book can evolve from small documents, thereby making the barrier for book writing much smaller. Also, several appealing ebook formats can be produced, both for the book and the individual chapter documents. The chances that your students read a chapter on the bus becomes larger if the chapter is available as attractive, screen-fit Bootstrap pages on the smart phone than if you just offer the classic LaTeX PDF which actually requires a big screen or a printer.

Implementation of point 1 and 2 is not trivial and requires some rules that might not feel natural at first sight in the setup. Writing a book soon becomes a technically and mentally complex task, just like developing a software system. For the latter people have invented a lot of sophisticated technologies and best practices to deal with the complexity. The present setup for books is a similar collection of my own technologies and best practices, developed from writing thousands of pages. In particular, the setup has been successfully used for the large-scale 900-page Springer book "A Primer on Scientific Programming with Python" [**?**] (individual chapters of this book, e.g. [**?**], can be examined online in various ebook formats) as well as for books in the works[2].

To use this setup, just clone the repository[3] and you have the directory structure, the scripts, and example files to get started with a book project at once! The source files for this book (especially in `doc/src/chapters/rules`) constitute nice demonstrations for learning about basic and advanced DocOnce writing techniques.

April 2015 *Hans Petter Langtangen*

[2] `http://hplgit.github.io/num-methods-for-PDEs/doc/pub/index.html`

[3] `https://github.com/hplgit/setup4book-doconce`

Contents

Chapter 1
Introduction and Motivation

In this chapter we provide a brief introduction to heart anatomy and physiology, to serve both as motivation and background material for the computational models presented in subsequent chapters. The description is intentionally kept brief, only introducing the key concepts required to understand the mathematical models. For a more detailed and complete overview of heart physiology, the reader is referred to a text book in the field, for instance [**?**].

1.1 Structure of the heart and cardiac muscle

1.1.1 Heart anatomy and mechanical function

The heart is a mechanical pump, which, in spite of its many associations to human emotions, serves the single purpose of pumping blood through the body. The pumping is achieved by a rhythmic, synchronized contraction of the heart muscle, and represents a tremendous physical effort as well as a fine-tuned interplay of mechanical, electrophysiological and neuro-hormonal factors. The heart is made up of four chambers, illustrated in Figure (xxx). The right and left ventricles constitute the main pumping chambers of the heart, while the two atria serve as primer pumps that improve the filling and thereby the pumping efficiency of the ventricles. An illustration of the cardiovascular system is shown in Figure xxx. Oxygen-poor blood from the vena cava enters the right atrium, then flows through the tricuspid valves into the right atrium, and is pumped via the pulmonary valve into the pulmonary circulation for oxygenation. After passing through the lungs, the now oxygen-rich blood returns to the heart via the pulmonary veins, enters the left atrium, and further into the left ventricle via the mitral valve. From the left ventricle the blood flows through the aortic valve into the aorta, and after several generations of branching vessels it reaches the capillaries, where

oxygen, nutrients and waste products are exchanged with the tissues. On the downstream side the capillaries merge into venules, which in turn are merged into larger and larger veins. Finally, the blood reaches the vena cava and flows back to the right ventricle to complete the cycle.

The pulmonary circulation (lungs) is a low-resistance system that operates under low pressure, while a much higher pressure is required to drive the flow through the higher resistance of the systemic circulation. The anatomy of the heart reflects this difference in blood pressure, with the left ventricle being thick-walled with a nearly circular cross section, and the more thin-walled right ventricle wrapped around it, see Figure (xxx).

1.1.2 Structure of cardiac muscle tissue

From a mechanical viewpoint, the heart tissue has two main constituents; the cardiomyocytes and the extracellular matrix. The cardiomyocytes make up about xx% of cardiac tissue, and are the muscle cells responsible for active contraction and performing work. The myocytes are roughly cylindrical in shape, with a length of about 100μm and diameter 10μm. They have a distinct orientation, which makes both the passive and active mechanical properties of the heart tissue highly anisotropic. The muscle cells line up end-to-end to form a fibrous tissue structure, although there are no long muscle fibers as seen in skeletal muscle. The orientation of the myocytes varies through the heart, as illustrated in Figure (xxx) for the left and right ventricle. The orientation is roughly helical, with the myocytes being aligned with the endocardial (inner) and epicardial (outer) surfaces, and forming an angle α with the cross-sectional plane. The angle varies approximately linearly from an endocardial value α_{endo} to the epicardial value α_{epi}, with typical values for human being XX and XX degrees, respectively. The cardiomyocytes are held together and supported by the extracellular matrix. The matrix is primarily made up of collagen, and contributes substantially to the passive mechanical properties of the tissue.

The pumping function of the heart is caused by the cyclic stretching and shortening of the myocytes, which in turn is driven by mechano-chemical processes in tiny sub-cellular structures called sarcomeres. In physical modeling terminology, the mechanics of the heart is truly a multiscale phenomenon. Each sarcomere is approximately XX μm long and has a diameter of around XX μm, and they are connected end-to-end into myofibrils, which are bundled together and fill most of the internal volume of the cardiac myocytes, as illustrated in Figure xxx.

Moving further down in physical scales, the sarcomeres are made up of overlapping thick and thin filaments, see Figure xxx. The thick filaments are made up of the protein xxx

The extracellular matrix is primarily made up of collagen,

Outline of muscle tissue organization;

- Overview of tissue structure
- Overview of cardiomyocyte structure, introducing the contractile proteins
- The extracellular matrix

1.2 The mechanics of heart contraction

Brief overview of the pumping function of the heart viewed as a mechanical multi-scale problem. A top-down view may be most illustrative, linking the different phases of the heart cycle (PV-loop, Wiggers diagram) to the mechanics of the tissue, the myocyte, and the sub-cellular structures.

1.3 Computational mechanics challenges

From a viewpoint of computational mechanics, outline the most important challenges of modeling heart mechanics.

1.3.1 Computational challenges of multiscale problems

As outlined above, the pumping of the heart is a multiscale physical phenomenon, where the macroscale function is directly linked to processes occuring on scales of μm or even nanometers. Defining models of such processes that are suitable for solving on a computer is highly non-trivial, as it involves capturing the essential features on one scale that are transfered to the scale above, without fully resolving the finer scales. For instance, while it may be possible to build a detailed model of of the protein interactions in a single sarcomere, there are thousands of sarcomeres in each myocyte, and up to 10 billion myocytes in a human heart. Resolving the fine details of each individual sarcomere in a computational model is obviously neither possible nor desirable, as the function of a single sarcomere, or even a few myocytes, will have no impact on the organ-scale pumping function. Rather, we are interested in building models that capture the essential details of the cellular and sub-cellular mechanisms, and how they are coupled to function and feedback mechanisms on the larger scales.

To model the effects of micro-scale details on larger scales we will apply a homogenization procedure, which is in principle similar to the approach used in continuum mechanics in order to view fluids and solids as continuous media rather than a large number of individual molecules. We will apply the same

principle to view the cardiac tissue as a continuum, neglecting the discrete, cell-based nature of the tissue. Physical quantities will be represented as continuous fields, and the net effect of micro-scale physical processes will also be represented in this way. For instance, a continuous field variable may represent the force developed by the sarcomeres, an approximation which hides the fine-scale details but allows (...).

Although the continuum approach to multiscale modeling is a considerable simplification compared with modeling each individual sarcomere or cell,

models of the pumping heart are true multiscale models, Referring to the outline of heart mechanics as a multiscale problem in Section 1.2, outline current modeling paradigm and the general computational challenges related to solving multiscale, multiphysics problems.

1.3.2 Mechanics of soft tissues

Outline classical aspects known to be challenging in continuum mechanics, and describe how they are present in models of passive muscle tissue:

- large deformations
- Non-linear material behavior
- Incompressibility and related numerical problems
- High anisotropy
- Uncertainty and variability in material parameters

1.4 Heart disease and mechanical dysfunction

Some re-organization is possible here, maybe placing this part before the outline of the mechanical problem.

- Brief summary of heart disease in general
- Outline selected heart problems where mechanical dysfunction of the heart muscle is an important factor. Of course, the distinction is not entire clear, but this would exclude severe arrhytmia and direct effects of valve dysfunction, but include heart failure and remodeling driven by load imbalance caused by electrical dyssynchrony or valve problems.

1.5 Outline and scope of the book

Should possibly (probably) be moved to a preface. Outline the book's content, focus and intended audience, and, most importantly, list the many important topics that will not be covered by the book.

Chapter 2
Introduction to Non-Linear Solid Mechanics

In this chapter we give a brief introduction to fundamental concepts of continuum mechanics, with particular focus on theory and tools relevant for large-deformaiton solid mechanics. We will introduce the important concepts of *stress* and *strain*, derive *balance equations* from fundamental mechanical principles, and introduce *constitutive laws* that relate deformation (strain) to internal forces (stress) for simple materials. More advanced material laws, applicable to the complex non-linear behavior of heart muscle tissue, will be introduced in Chapter **??**.

2.1 Fundamental concepts of continuum mechanics

2.1.1 The continuum hypothesis

Biological tissue, including cardiac muscle, is a complex mix of cells, fluids, and extracellular matrix proteins, and capturing the full details of this tissue composition in a computational model would be very challenging. Even if we only focus on representing the muscle cells, there are about ten billion of these in a human heart, and representing all of them will lead to extremely expensive computations. Fortunately, we are normally not interested in the mechanical properties of a single cell, only in their collective mechanical behavior, and in this case classical *continuum mechancis* provides a suitable modeling framework.

The foundation of continuum mechanics is to view the physical world as continuous media, and neglect the discrete atomic and molecular nature of all materials. This approach is of course quite intuitive, and matches well with our general perception of the world, but from a theoretical viewpoint it involves a number of key assumptions. Consider for instance a fundamental

physical quantity such as density of mass, which is commonly viewed as a property of a material. How can we define the density $\varrho(\mathbf{x},t)$ as a continuous field, for a material which is mostly void space with some sparsely distributed molecules or atoms? The solution is to define $\varrho(\mathbf{r},t)$ as a quantity that is averaged over a volume containing a large number of molecules. We pick a small volume ΔV, compute its mass ΔM, and define the average density $\varrho^{(a)} = \Delta M/\Delta V$. Viewed as a continuous field, $\varrho(\mathbf{x},t)$ is the average density in a small volume around the point $\mathbf{x}$ at time t, and this definition is implied for all the continuous field quantities introduced in this book. This theoretical definition will not have any practical implications for the models considered here, but it is still worth keeping in mind for all practitioners of computational biology. In physics, this process of homogenization is theoretically sound if we can choose the volume ΔV so that it contains a large number of molecules, but is also much smaller than the scale of the phenomenon under study. This condition is usually easy to satisfy in classical continuum mechanics. However, to be applicable in biology the averaging should be done over a large number of *cells* rather than molecules, which may be problematic for some applications.

2.1.2 Lagrangian and Eulerian description

In continuum mechanics, an important distinction is made between a *Eularian* and *Lagrangian* description of field quantities. If we consider for instance a velocity field $v(\mathbf{x},t)$, the difference between the Lagrangian description $v_L(\mathbf{X},t)$ and the Eularian description $v_E(\mathbf{x},t)$ can be summarized as follows:

- $\mathbf{v}_E(\mathbf{x},t)$: The velocity of the continuum *particle* that is located at the spatial point $\mathbf{x}$ at time t
- $\mathbf{v}_L(\mathbf{X},t)$: The velocity of the continuum particle that was *initially* located in the point $\mathbf{X}$

Note the important distinction between the spatial coordinates $\mathbf{x}$ and the initial (or material) coordinates $\mathbf{X}$. The $\mathbf{X}$ should be interpreted as particle labels, and the Lagrangian description works by tracking these continuum particles over time. The Lagrangian coordinates $\mathbf{X}$ are often referred to as *material coordinates*, while $\mathbf{x}$ are the *spatial coordinates*. The difference between the two formulations can be illustrated further by considering the partial derivatives of the two fields $\mathbf{v}_E(\mathbf{x},t)$ and $\mathbf{v}_L(\mathbf{X},t)$. The correct physical interpretation of $\partial\mathbf{v}_E/\partial t$ is as the rate of change in the velocity of particles at a fixed point in space;

$$\frac{\partial \mathbf{v}_E}{\partial t} = \lim_{\Delta t \to 0} \frac{\mathbf{v}_E(\mathbf{r}, t+\Delta t) - \mathbf{v}_E(\mathbf{r},t)}{\Delta t}.$$

Here, it is important to note that $\mathbf{v}_E(\mathbf{r}, t+\Delta t)$ and $\mathbf{v}_E(\mathbf{r}, t)$ are the velocities of two different particles. Therefore, although we usually get acceleration as the time-derivative of velocity, in this case we do *not* obtain the acceleration of a physical continuum particle. On the other hand, the Lagrangian description $\mathbf{v}_L(\mathbf{X}, t)$ follows individual particles by defnition, so the partial derivative $\partial \mathbf{v}_L / \partial t$ becomes the physical acceleration of an individual continuum particle. The distinction is important, in particular in fluid mechanics and large-deformation solid mechanics. As can be inferred from this simple example, the Lagrangian formulation may be seen as being closer to the intuitive physics, but it will often lead to more complex mathematical relations. Also, for fluid mechanics applications it is usually inconvenient and not of interest to track all individual particles.

Of course, the Lagrangian and Eulerian description of a field are supposed to describe the same physical quantity, and we can map between the two formulations by expressing the spatial position of a particle as a function of time and its initial position;

$$\mathbf{x} = \mathbf{x}(\mathbf{X}, t).$$

From this mapping we can easily define the velocity and acceleration of individual particles in a Lagrangian description;

$$\mathbf{v}(\mathbf{X}, t) = \frac{\partial \mathbf{x}}{\partial t}, \quad \mathbf{a}(\mathbf{X}, t) = \frac{\partial \mathbf{v}}{\partial t}.$$

Similarly, the acceleration of a continuum particle in a Eulerian description can be obtained by inserting (2.1.2) and using the chain rule:

$$\begin{aligned} \mathbf{a}(\mathbf{x}, t) &= \frac{d\mathbf{v}(\mathbf{x}(\mathbf{X}, t), t)}{dt} \\ &= \frac{\partial \mathbf{v}(\mathbf{x}, t)}{\partial x} \frac{\partial \mathbf{x}(\mathbf{X}, t)}{\partial t} + \frac{\partial \mathbf{v}(\mathbf{x}, t)}{\partial t} \qquad = \mathbf{v} \cdot \nabla \mathbf{v} + \frac{\partial v}{\partial t}. \end{aligned}$$

We see that this definition of acceleration as the *total derivative* has two components; one is the time rate of change of velocity in a spatial point $\mathbf{x}$, and the other is the change in velocity as particles move to a position with higher velocity. The formula is essential in fluid dynamics, and is therefore included here for completeness, but it is usually not needed in solid mechanics applications.

2.2 Deformation and strain

The Lagrangian description is often preferred for solid mechanics applications. In a typical solid mechanics problem we know the original shape and

position of a continuum body, apply some static or dynamic loads, and then want to compute the resulting shape, deformation, and internal forces (stresses) in the body. The shape of the deformed body at any given time is given by the spatial coordinates $\mathbf{x}(\mathbf{X},t)$, so this field is typically a central variable of interest. However, instead of solving for the spatial coordinates directly, it is common to define the *displacement field* $\mathbf{u}$ as the primary unknown variable. The displacement is given by

$$\mathbf{u} = \mathbf{x}(\mathbf{X},t) - \mathbf{X},$$

and simply describes how much a given point $\mathbf{X}$ in the original configuration has moved. The motivation for introducing the displacement field is that we want to introduce measures of *deformation*, which we will later use in material laws that link deformation with internal forces (stresses) acting on the material. Since $\mathbf{u}$ describes how much each point $\mathbf{X}$ has moved, it is a good starting point for quantifying deformation, but it is not quite what we need. The reason is that we want a measure of deformation that can be directly related to internal forces in the continuum. Such internal forces are related to change of shape of the continuum, which can easily be illustrated by bending a thin structure such as a rod or a plate. We apply a bending force, the structure visibly changes its shape, and we can intuitively assume that there are internal forces acting inside the structure, effectively opposing and balancing the applied bending force. The displacement field will include all the relevant information about such a deformation, including the change of shape. However, it also includes components of *rigid body motion*, which do not give rise to internal forces in the material, and are therefore not relevant input quantities in material laws. This can be illustrated intutively by a body subject to a constant displacement field, for instance $\mathbf{u} = (1,0,0)$, i.e., moving the entire body one length unit along the x-axis. Such a translation will obviously not introduce any internal forces in a body, and the discplacement field itself is therefore not a good candidate for relating deformation to internal forces. More generally, a displacement field describing rigid body motion can be described mathematically as

$$\mathbf{u} = \mathbf{u}_0 + \mathbf{R}\mathbf{X}, \tag{2.1}$$

where $\mathbf{u}_0$ is a constant and $\mathbf{R}$ is an orthogonal *rotation tensor*. The first term on the right hand side represents a *rigid translation*, while the second term is a *rigid body rotation*. Since neither rigid translation nor rigid rotation gives rise to internal forces, we want to define measures of deformation where all components on the form in (2.1) are eliminated. To obtain such a quantity, we start by taking the gradient of the displacement field with respect to the material coordinates $\mathbf{X}$, to define (NBNB feil!!)

$$\mathbf{F} = \frac{\partial \mathbf{u}}{\partial \mathbf{X}} = \nabla \mathbf{u}.$$

The new quantity $\mathbf{F}$ is called the *deformation gradient*, and is a central quantity in large-deformation solid mechanics. It serves both as a measure of deformation, quantifying the change of shape as a body deforms, and also to map infitesimal quantities back and forth between the reference and deformed configuration. We will come back to the latter use of $\mathbf{F}$ later, for now we focus on its role as a measure of deformation.

We see that for the rigid motion displacement field in (2.1), we have $\mathbf{F} = \mathbf{R}$, so the translational components have been removed, and we are one step closer to defining a quantity that measures pure change of shape. To remove the rotational components as well, we may apply the *polar decomposition theorem* (REFERENCE), which states that any tensor $\mathbf{F}$ can be decomposed as follows:

$$\mathbf{F} = \mathbf{R}\mathbf{U} = \mathbf{v}\mathbf{R}.$$

Here, $\mathbf{U}, \mathbf{v}$ are symmetric tensors, $\mathbf{U} = \mathbf{U}^T$, and $\mathbf{R}$ is an orthogonal pure rotation tensor. Since $\mathbf{R}$ is orthogonal, we have

$$\mathbf{F}^T\mathbf{F} = (\mathbf{R}\mathbf{U})^T(\mathbf{R}\mathbf{U}) = \mathbf{U}^T\mathbf{R}^T\mathbf{R}\mathbf{U} = \mathbf{U}^T\mathbf{U},$$

and we see that by multiplying $\mathbf{F}$ with its transpose we have eliminated all the rotational components. The resulting tensor $\mathbf{C} = \mathbf{F}^T\mathbf{F}$ is called the *right Cauchy-Green tensor*, and is a commonly used measure of deformation in large-deformation solid mechanics.

2.2.1 Mapping the reference to the undeformed configuration

As noted above, a central use of the deformation gradient tensor in large-deformation mechanics is to map back and forth between the undeformed and deformed configuration of a continuum. The reason is that the deformed configuration is unknown, and it is therefore convenient to formulate the problem relative to the undeformed configuration. To do this, we need to map relevant quantities, typically infinitesimal *line segments*, *surface elements*, and *volumes* between the reference and the deformed condfiguration. By using the definition of $\mathbf{F}$ as the gradient of the mapping $\varphi(\mathbf{X}, t)$ (NB ikke introdusert), it can be shown that an infinitesimal line segment $d\mathbf{X}$ in the reference configuration is mapped to the line segment

$$d\mathbf{x} = \mathbf{F}d\mathbf{X} \tag{2.2}$$

after the deformation. Later, we will also need to map infinitesimal area segments, and in particular area segments with an orientation, i.e., a *surface element* $d\mathbf{S} = dS\mathbf{N}$, where dS is the area and $\mathbf{N}$ its surface normal. The mapping of such surface elements between the reference and deformed state

is according to Nanson's formula:

$$d\mathbf{s} = J\mathbf{F}^{-T}d\mathbf{S}, \tag{2.3}$$

where $d\mathbf{s} = ds\mathbf{n}$ is the deformed surface element, with area ds and unit normal $\mathbf{n}$, and $J = \det \mathbf{F}$ is the determinant of $\mathbf{F}$, which is also the central quantity describing volume change;

$$dv = JdV. \tag{2.4}$$

The formulas (2.2)-(**??**) will be used extensively throughout this book. For a detailed derivation of the formulas we refer to a comprehensive text book on continuum mechanics, for instance [**?**].

With the mapping (2.2) at hand, we can introduce an alternative derivation of $\mathbf{C}$, which makes it more evident that it represents a change of shape. Consider a line segment $d\mathbf{X}$ in the reference configuration, which deforms to $d\mathbf{x}$ after the deformation. A measure of shape change can be derived by quantifying the *length change* of such a line segment as the body deforms, since for a rigid mody motion $||d\mathbf{x}|| = ||d\mathbf{X}||$. We have

$$\begin{aligned} ||d\mathbf{x}||^2 - ||d\mathbf{X}||^2 &= d\mathbf{x}^T d\mathbf{x} - d\mathbf{X}^T d\mathbf{X} \\ &= ((\mathbf{F}d\mathbf{X})^T \mathbf{F}dX - d\mathbf{X}^T d\mathbf{X}) = ((d\mathbf{X})^T CdX - d\mathbf{X}^T d\mathbf{X}) \\ &= (\mathbf{C} - \mathbf{I})d\mathbf{X}^T d\mathbf{X}, \end{aligned}$$

which shows that all the information to compute the length change of $d\mathbf{X}$ is held in the tensor $\mathbf{C}$. From this derivation we can also motivate an alternative measure of deformation, the so-called *Green-Lagrange strain tensor*, defined by

$$\mathbf{E} = \frac{1}{2}(\mathbf{C} - \mathbf{I}). \tag{2.5}$$

Both $\mathbf{C}$ and $\mathbf{E}$ are widely used in material laws describing large-deformation solid mechanics. One difference between them is that $\mathbf{E}$ is an actual *strain*, because by defition a strain is zero when there is no deformation. The right Cauchy-Green tensor for no deformation is $\mathbf{C} = \mathbf{I}$, so the right Cauchy-Green tensor is by definition not a strain, although it is a precise measure of change of shape that is suitable for use in material laws relating deformation to internal forces.

Many will be familiar with the small-deformation strain tensor used in linear elasticity, which is often formulated in as

$$\epsilon_{ij} = \frac{1}{2}(\frac{\partial u_i}{\partial x_j} + \frac{\partial u_j}{\partial x_i}),$$

or in the notation used so far in this chapter;

$$\epsilon = \frac{1}{2}(\nabla u + \nabla u^T).$$

If we expand the Green-Lagrange strain tensor in (2.5) using the definition of $\mathbf{C}$ and $\mathbf{F}$, we get

$$E_{ij} = \frac{1}{2}\left(\frac{\partial u_i}{\partial X_j} + \frac{\partial u_j}{\partial X_i} + \frac{\partial u_i}{dX_j}\frac{\partial u_j}{dX_i}\right).$$

(We use the index notation to make clear the distinction between $\partial/\partial x$ and $\partial/\partial X$.) For small deformations the linear terms dominate the quadratic ones, so we can set $\frac{\partial u_i}{\partial X_j}\frac{\partial u_j}{\partial X_i} \approx 0$. Furthermore, for small deformations the distinction between $\mathbf{X}$ and $\mathbf{x}$ becomes insignificant, so the Green-Lagrange strain reduces to the familiar small-deformation strain tensor. This similarity also helps to explain the factor $1/2$ appearing in the the Green-Lagrange strain, since it makes it more closely resemble the small-strain tensor and makes the physical interpretation of its components more intuitive.

Invariants of tensors. All the strains and deformation tensors introduced so far involve gradients, i.e., their components are computed from derivatives of the displacement field with respect to spatial or material coordinates. Therefore, changing the coordinate system used, for instance rotating the axes a given angle, will change the components of the tensors. This property is quite natural, and does not represent a problem in itself, but since the strain and deformation tensors represent physical quantities, they should have some key characteristics that are independent of the coordinate system used. Such physical characterization of a tensors is obtained by computing its eigenvalues and eigenvectors. These are properties that are independent of the coordinate system used, and characterize the principal directions and principle values of a given tensor quantity. Eigenvalue analysis to determine the principal directions of stresses and strains are usually a key part of solid mechanics analysis, but it is normally less relevant in soft tissue mechanics and will therefore not be discussed here. However, closely related to the eigenvalues are the three so-called *principal scalar invariants*, wich for a general tensor $\mathbf{A}$ are defined as

$$I_{\mathbf{A}} = tr\mathbf{A}, \quad II_{\mathbf{A}} = \frac{1}{2}((tr\mathbf{A})^2 - tr(\mathbf{A}^2)), \quad III_{\mathbf{A}} = \det\mathbf{A}.$$

The invariants are the coefficients of the characteristic polynomial of $\mathbf{A}$, which has the eigenvalues of $\mathbf{A}$ as roots. Similar to the eigenvalues, the principal invariants are independent of coordinate transformations, and characterize the physical nature of a tensor. This property makes them convenient to use in material laws that relate strains to internal forces (stresses), and for this reason it is important to have a fundamental understanding of them. We shall see examples of material laws involving strain invariants later in this chapter, and in Chapter **??** we shall also define additional (pseudo-)invariants that are suitable for characterizing anisotropic materials.

2.3 The concept of stress

So far in this chapter, we have introduced a precise mathematical description of deformation, and arrived at quantities that are precise measures of change of shape. An important motivation for introducing these quantities was to use them in material laws that relate deformation to internal forces in the continuum, but we have so far not provided a precise definition of these internal forces. To introduce this topic, we first consider two types of forces that can act on a continuum body; *body forces* and *surface forces*. Body forces are distant forces that act on every point of a continuum body, with gravity being the most obvious example. For a body force $\mathbf{b}$ acting on a body, the total force $\mathbf{B}$ is

$$\mathbf{B} = \int_{\text{body}} \mathbf{b} dV,$$

where $\mathbf{B}$ has units of force, and $\mathbf{b}$ is force per volume.

The other type of force, surface forces, act on the surface of a body or on the imaginary surface of a part of a body. Such forces are conveniently quantified by the *stress* $\mathbf{s}(\mathbf{x}, t)$, which is a vector quantity defined as force per area. The total surface force acting on a body is given by

$$\mathbf{S}(\mathbf{x}, t) = \int_{\text{surface}} \mathbf{s}(\mathbf{x}, t) dA.$$

Stress is force per unit area, and is a vector quantity having the same direction as the force. However, it is important to remark that the stress vector depends on the orientation of the area considered. That is, the stress at a point on a surface depends on the location of the point, and on the orientation of the surface at that point. As a simple illustration, consider the stress in a rod with cross-sectional area A, subject to a stretching force F, see Figure 2.1. From simple equilibrium considerations, the stress vector on a cross-sectional surface must have magnitude F/A, and is directed along the length of the rod. On a surface parallel to the length of the rod, the stress vector will be zero, since no forces act in the transverse direction. In general, we need to know the surface orientation, i.e., the surface normal $\mathbf{n}$, to compute the stress vector.

For the stress vectors and the surface orientation considered in this simple example, all the stress vectors acted perpendicular to the surface considered. However, this is not always the case, and in general there will be forces acting both parallel and tangential to the surface of interest. In the example in Figure 2.1, this would be the case if we for instance considered a surface at a 45 degree angle to the length direction of the rod. In this more general case, we can decompose the stress vector into *normal stress* σ_N and *shear stress* σ_T, where the latter describes stresses tangential to the surface, see

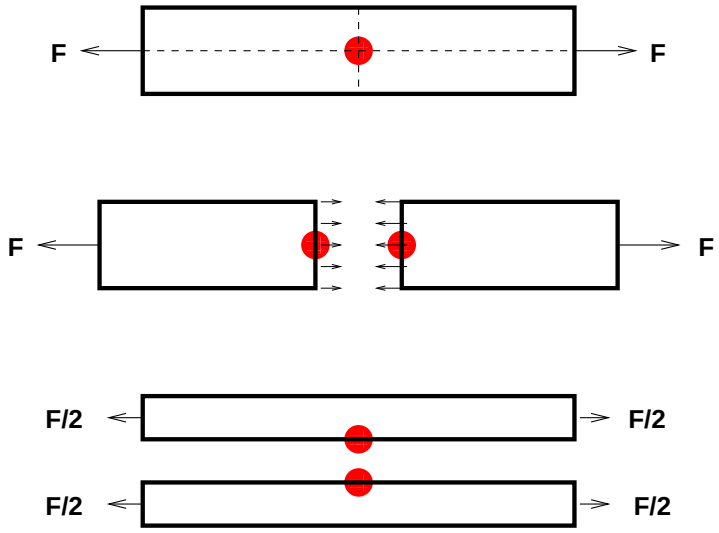

Fig. 2.1 Illustration of stress resulting from a stretching force F applied to a rod. The stress vector in the bullet point will be different depending on the orientation of the surface we are looking at.

Figure 2.2. The normal stress is given by $s_N = \mathbf{s} \cdot \mathbf{n}$, and the normal stress vector $\mathbf{N} = \sigma_N \mathbf{n}$, while the shear stress vector is $\mathbf{T} = \mathbf{s} - \mathbf{N}$ and $\sigma_T = ||\mathbf{T}||$

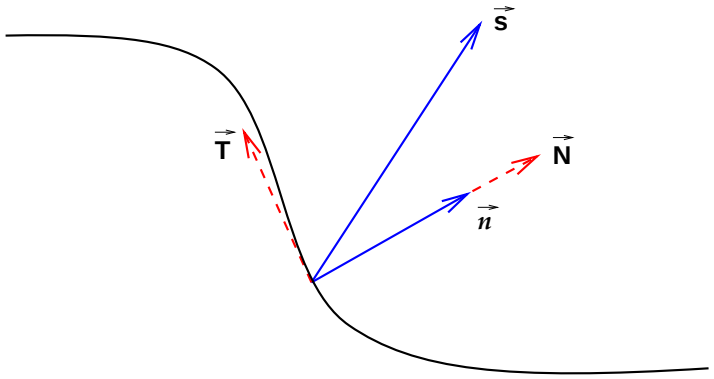

Fig. 2.2 Sketch of how an stress vector **s** on an arbitrary surface is decomposed into normal stress **N** and shear stress **T**.

2.3.1 The Cauchy stress tensor

So far we have merely stated that the stress on a surface depends on the surface orientation, without considering *how* it depends. Fortunately, the dependence is quite simple, as stated by a famous theorem known as Cauchy's first law, or Cauchy's stress theorem. This theorem introduces the fundamental quantity known as the *stress tensor*, which is a symmetric second order with six independent components. In matrix form, it reads

$$\sigma = \begin{pmatrix} \sigma_{xx} & \sigma_{xy} & \sigma_{xz} \\ \sigma_{xy} & \sigma_{yy} & \sigma_{yz} \\ \sigma_{xz} & \sigma_{yz} & \sigma_{zz} \end{pmatrix}.$$

The theorem now states that if we know the six components of the stress tensor, we can compute the stress vector on any surface from the relation

$$\mathbf{s}(\mathbf{x}, t; \mathbf{n}) = \sigma(\mathbf{x}, t)\mathbf{n}(\mathbf{r}, t).$$

We see that $\mathbf{s}$ has a simple (linear) dependence on $\mathbf{n}$, and this relation is of crucial importance in the derivation of the fundamental equations of mechanics. The entries of the stress tensor have a physical interpretation, but most importantly they are ingredients in a tool (Cauchy's 1. law) for computing the stress vector at an arbitrary surface. The physical interpretation is as follows; σ_{ii}, i is normal stress on a plane $i = \text{const}, i = x, y, z$, while σ_{ij} is shear stress in j direction on a plane $i = \text{const}, i, j = x, y, z$.

To revisit the simple example of stretching a rod above, how can we find the stress tensor in this case? Usually, computing the stress tensor involves solving a PDE with associsated boundary conditions, but in this simple case we mauy use physical reasoning to guess at a stress tensor.

Cutting the body along coordinate planes ($x = \text{const}$, $y = \text{const}$, $z = \text{const}$)

$$\sigma = \begin{pmatrix} F/A & 0 & 0 \\ 0 & 0 & 0 \\ 0 & 0 & 0 \end{pmatrix}.$$

How can we know that this guess is correct? Physical reasoning indicates such a stress tensor, and we can compute the resulting stress vector on cross-sectional and longitudinal surfaces to verify that we get what we expect. However, in general only the solution of a full model for elastic deformation can tell if our assumption of σ is correct. In classical mechanics, before computers dominated the field, guesses based on physical reasoning were typically required to treat the problem analytically. Today, such guesses remain crucial to assess whether numerical results are reasonable.

2.3.2 Large-deformation stress tensors

The Cauchy stress tensor introduced above is sometimes referred to as the *true stress*, and is the most important physical quantity describing internal forces in a continuum. However, in the context of large-deformation solid mechanics it has some limitations, which have motivated the introduction of alternative stress tensors. We recall that stress is a vector quantity defined as force divided by area, but in general the deformed configuration is unknown and therefore we don't know this area. In the case of small deformations the distinction is not important, since the area does not change much from the reference configuration, but when deformations are large the area can change significantly. As an illustration, think of the uni-axial stretch of the rod above. The rod will become slightly longer as we apply the force, and intuitively it will also get a little thinner. If it is a steel rod that you pull with your hands, it will most likely be difficult to notice any change in length or diameter, but if the rod is a rubber band you can easily see that it gets thinner as it is stretched. The cross-sectional area changes significantly, and to get correct stress calculations in large-deformation problems we need to account for this change. The challenge is that we don't know the deformed geometry until we have solved the problem, and in order to solve the problem we need to be able to calculate the stress. Iterative solution processes may be applied, where a problem is formulated in terms of the Cauchy stress, and then the geometry is iteratively updated, but it is usually more convenient to reformulate the problem relative to the reference configuration. For this purpose we need alternative stress tensors, in addition to the large-deformation deformation measures introduced previously.

One intuitive way to define a stress tensor without knowing the deformed geometry is to consider the force acting on an arbitrary surface in the deformed configuration, which can be computed using the Cauchy stress tensor. We can then map the surface back to the undeformed configuration, and define a stress tensor there so that the two forces are identical. Using (2.3), we have

$$\mathbf{f} = \sigma \mathbf{n} a = \sigma J \mathbf{F}^{-T} \mathbf{N} A, \tag{2.6}$$

where $a, \mathbf{n}$ and $A, \mathbf{N}$ are the area and surface normal of the deformed and undeformed surface, respectively. We now simply define a new stress tensor as

$$\P = J\sigma \mathbf{F}^{-T}. \tag{2.7}$$

which ensures that the forces resulting from this stress tensor in the undeformed configuration are the same as the forces resulting from the Cauchy stress tensor in the deformed configuration. The new quantity $\mathbf{P}$ is called the *first Piola-Kirchhoff stress tensor*, and is a commonly used stress measure in large-deformation solid mechanics. It is important to note, however, that the Cauchy stress is still the quantity that describes the *actual* stress state in the deformed body, and this is usually the most important quantity of interest.

The first Piola-Kirchhoff stress is simply a convenient tool to formulate and solve the mechanics problem, since it is enables a consistent formulation of the stress without knowing the deformed configuration of the body.

Unlike the Cauchy stress, the first Piola-Kirchhoff stress is not symmetric, which is seen from (2.7) and the fact that $\mathbf{F}$ is not symmetric. An alternative stress tensor can be derived by mapping the force $\mathbf{f}$ in (2.6) back to the reference configuration using (2.2). We get

$$\mathbf{f}_0 = \mathbf{F}^{-1}\mathbf{f} = \mathbf{F}^{-1}\sigma\mathbf{n}a = \mathbf{F}^{-1}\sigma J\mathbf{F}^{-T}\mathbf{N}A. = \mathbf{S}\mathbf{N}A.$$

and define the new stress tensor to be $\mathbf{S} = J\mathbf{F}^{-1}\sigma\mathbf{F}^{-T} = \mathbf{F}^{-1}\mathbf{P}$. This tensor is called the *second Piola-Kirchhoff stress tensor*, which is symmetric and therefore in some cases more convenient to use than the first Piola-Kirchhoff tensor. While the Cauchy stress tensor relates forces and surfaces in the deformed configuration, the first Piola-Kirchhoff stress relates forces in the deformed configuration to undeformed surfaces, and the second Piola-Kirchhoff stress relates forces and surfaces both in the undeformed configuration. However, only the Cauchy stress has a meaningful physical interpretation, while the two others are useful tools to formulate and solve the mechanics problem. A number of alternative stress measures have been introduced for large-deformation solid mechanics, but the first and second Piola-Kirchhoff stresses are probably the most widely used. They will both be used extensively throughout this book.

2.3.3 Balance equations

Present a compact derivation of the fundamental laws of motion, based on conservation of linear momentum.

- Euler description, Cauchy stress
- Lagrange description, Piola-Kirchoff stress
- Discuss the relative significance of the terms, motivate the quasi-static approach and the neglection of body forces
- Discuss the general nature of the equation, and relate this to the mismatch between number of equations and unknowns. This motivates the need for constitutive models.

The three fundamental laws

- Conservation of mass
- Conservation of momentum (Newton's second law)
- Conservation of energy (The first law of thermodynamics)

Expressions of the fundamental laws

We shall express the three fundamental laws mathematically in three forms

- Integral form
- Conservative differential form
- Simplest (standard) differential form

We will mainly apply the standard differential form, but the others are used in derivations.

Structure of derivations

- State the law with words
- Express the law for a *material volume*
- Use Reynolds' transport theorem to remove time-dependent integration domains

⇒ Integral form

- Transform surface integrals to volume integrals by Gauss' theorem

⇒ Conservative differential form

- Expand terms and simplify

⇒ Simplest (standard) differential form

The equation of motion

Newton's 2nd law:

$$\frac{d\mathbf{I}}{dt} = \mathbf{F}$$

where $\mathbf{I}$ is momentum:

$$\mathbf{I} = \int_V \varrho \mathrm{d}V$$

$\mathbf{F}$ is the total external force: surface forces + body forces

Two types of forces

- surface forces

$$\int_{\partial V} \sigma \cdot \mathbf{n} dS$$

- body forces (e.g. gravity)

$$\int_V \varrho \mathbf{b} dV$$

2.3.4 The Boundary Value Problem

A suitable starting point when modeling the deformation of a continuum, is Cauchy's first equation of motion, which may be expressed as [**?**]

$$\nabla \cdot \sigma + \mathbf{b} - \varrho \ddot{\mathbf{u}} = \mathbf{0}.$$

Here, σ is the Cauchy stress tensor, $\mathbf{b}$ is a vector representing the body forces per unit volume, ϱ is the density, and $-\varrho\ddot{\mathbf{u}}$ characterizes the inertia force per unit volume. In this equation all terms refer to the deformed configuration. We remark that the Cauchy stress tensor is symmetric, i.e. $\sigma^T = \sigma$, resulting in a maximum of six independent stress components in the general three-dimensional (3D) case [**?**].

One of the goals of the present work is to model the mechanics of the heart muscle. Then, the contributions from body forces and the inertia term are believed to be much smaller than the contribution from the term containing internal stresses. Hence, the body force and the inertia terms may be neglected, yielding

$$\nabla \cdot \sigma = \mathbf{0}. \tag{2.8}$$

For this problem, a proper set of boundary conditions is [**?**]

$$\mathbf{u} = \bar{\mathbf{u}}, \qquad \text{on } \partial\Omega_u, \tag{2.9}$$

$$\mathbf{t} = \bar{\sigma} \cdot \mathbf{n}, \quad \text{on } \partial\Omega_\sigma. \tag{2.10}$$

In Section xxx we argued that it is convenient to refer all quantities to a reference configuration. In this configuration the simplified equation of motion (2.8) has the following equivalent counterpart,

$$\nabla_0 \cdot \mathcal{P} = \mathbf{0}, \tag{2.11}$$

where ∇_0 is the differentiation operator with respect to the undeformed configuration. Furthermore, the first Piola-Kirchhoff stress tensor in (2.11) can be replaced by the tensor product in (**??**), which gives

$$\nabla_0 \cdot (\mathcal{F}\mathcal{S}) = \mathbf{0}.$$

Similarly, the natural boundary condition (2.10) may be expressed by the equivalent traction force in the reference configuration,

$$\mathbf{T} = \bar{\mathcal{P}} \cdot \eta = \mathcal{F}\bar{\mathcal{S}} \cdot \eta = \mathcal{F}J\mathcal{F}^{-1}\bar{\sigma}\mathcal{F}^{-T} \cdot \eta = J\bar{\sigma}\mathcal{F}^{-T} \cdot \eta. \tag{2.12}$$

Here, η is the outward unit normal vector with respect to the reference configuration. The rest of the involved quantities have been defined above.

The traction forces in the two configurations, (2.10) and (2.12), are closely related. From Nanson's formula [**?**], we have that

$$\eta dS = J^{-1}\mathcal{F}^T \cdot \mathbf{n} ds,$$

where dS is an infinitesimal area in the reference configuration and ds is the corresponding area in the deformed configuration. Thus, the traction force on the area dS becomes

$$\mathbf{T}dS = J\sigma\mathcal{F}^{-T}\cdot\eta dS = J\sigma\mathcal{F}^{-T}J^{-1}\mathcal{F}^{T}\cdot\mathbf{n}ds = \sigma\cdot\mathbf{n}ds = \mathbf{t}ds. \tag{2.13}$$

From (2.13), we observe that the traction vectors in the material and deformed configurations are pointing in the same direction, but that the absolute values generally differ.

Summing up, we have the complete boundary value problem in the material configuration:

$$\nabla_0\cdot(\mathcal{F}\mathcal{S}) = \mathbf{0}, \qquad \text{on } \Omega, \tag{2.14}$$

$$\mathbf{u} = \bar{\mathbf{u}}, \qquad \text{on } \partial\Omega_u, \tag{2.15}$$

$$\mathbf{T} = J\sigma_0\mathcal{F}^{-T}\cdot\eta, \quad \text{on } \partial\Omega_\sigma. \tag{2.16}$$

In order to completely describe the problem under consideration, we need to define some material properties. Equation (2.14) is expressed by the deformation gradient and stresses. Stresses are related to strains, and the stress-strain relation defines the constitutive law for the material. Simple constitutive laws will be the topic of the next section, while the more complex models to describe actively contracting heart tissue are introduced in chapters 4 and 5.

2.4 Modeling material behavior

Give a general introduction to constitutive modeling, explicitly neglecting the complex behavior of the heart muscle and other soft tissues. For completeness and to increase the understanding of the balance equations presented above, describe the general behavior of fluids and solids, briefly list models for "advanced" solids (visco-elasticity, plasticity etc), and proceed to describe simpler elastic and hyperelastic models. This section has two purposes; (1) to give a soft introduction to material modeling before diving into the more complex and realistic case, and (2) to arrive at some fairly compact model problems that will be used to introduce the computational techniques in the next chapter.

2.4.1 Hyper-elasticity

Although it is clearly an approximation of the more complex reality, heart muscle and other soft tissues are usually modeled as *hyper-elastic* materials. A hyper-elastic material is simply defined as a material where the relation between stress and strain can be derived from a strain energy function. The strain energy function describing the elastic energy stored in the material, and hyper-elasticity is a generalization of linear elasticity to the case of large

deformations and non-linear material behavior. Many will be familiar with the famous Hooke's law, which gives a linear relation between stress and strain. Hooke's law exists in many forms, but for isotropic elastic materials one of the more well known formulations is

$$\sigma = \lambda tr(\varepsilon)\mathbf{I} + 2\mu\varepsilon, \tag{2.17}$$

where λ, μ are the Lamé constants. In its most general form, the *generalized Hooke's law* gives the relation between stress and strain as

$$\sigma = \mathbb{C}\epsilon, \tag{2.18}$$

where $\mathbb{C}$ is a fourth-order tensor. In index notation, the law is expressed as

$$\sigma_{ij} = C_{ijkl}\epsilon_{kl},$$

and since the indices run from 1 to 3, the tensor $\mathbb{C}$ can have at most 81 entries. Symmetry requirements reduce the number of independent constants to 21 in the most general case, and down to two in the case of isotropic materials.

Although strain energy functions are not commonly used for small deformations, a strain energy corresponding to the generalized Hooke's law can be expressed as

$$\Psi(\epsilon) = \frac{1}{2}\mathbb{C}\epsilon^2, \tag{2.19}$$

or for the isotropic case above as

$$\Psi(\varepsilon) = \frac{\lambda}{2}(tr(\varepsilon))^2 + \mu tr(\varepsilon^2). \tag{2.20}$$

We may observe that the stress-strain relations (2.17) and (2.18) can be obtained by differentiating the strain energy functions (2.19) and (2.20) with respect to the strain. This relation holds in general and is an important characteristic of strain energy functions and hyper-elastic materials;

$$\sigma = \frac{\partial \Psi}{\partial \varepsilon}. \tag{2.21}$$

When solving a mechanics problem, the quantities of interest are usually the stresses and strains, not the strain energy, and the stress-strain relation is the most useful and applicable characterization of material behavior. However, the strain energy is a convenient and compact way to express the material behavior of a hyper-elastic material, from which we can easily derive the relevant stress-strain relation from (2.21).

In large-deformation hyper-elasticity, the strain energy is usually written as a function of the Green-Lagrange strain or the Right Cauchy-Green tensor, and we recover second Piola-Kirchhoff stress by differentiation with respect to $\mathbf{E}$ or $\mathbf{C}$;

$$\mathbf{S} = \frac{\partial \Psi}{\partial \mathbf{E}} = 2\frac{\partial \Psi}{\partial \mathbf{C}}. \tag{2.22}$$

Note that the differentiation is performed with respect to all the strain components. On index form the relation is

$$S_{ij} = \frac{\partial \Psi}{\partial E_{ij}} = 2\frac{\partial \Psi}{\partial C_{ij}},$$

implying that we differentiate the scalar function Ψ with respect to the six independent components of $\mathbf{E}, \mathbf{C}$ to obtain the six entries of $\mathbf{S}$. Observant readers may now question why we get exactly the second Piola-Kirchoff stress by differentiating with respect to $\mathbf{E}$. The reason is that the second Piola-Kirchoff stress is *work-conjugate* with the Green-Lagrange strain. As noted above, a number of alternative stress tensors have been proposed in large-deformation mechanics, and there are also many work-conjugate pairs of stress and strain tensors. For instance, the first Piola-Kirchhoff stress is work conjugate to the deformation gradient F, so that the following relation holds;

$$\mathbf{P} = \frac{\partial \Psi}{\partial \mathbf{F}}. \tag{2.23}$$

We refer to [**?**] for a more detailed discussion of work-conjugate pairs and their physical interpretation.

A simple strain energy function for large deformations is obtained by replacing ε in (2.20) with the Green-Lagrange strain $\mathbf{E}$, to obtain the so-called Saint Venant-Kirchhoff material model;

$$\Psi(E) = \frac{\lambda}{2}(tr(E))^2 + \mu tr(E^2).$$

Differentiating with respect to E gives the stress-strain relation

$$S = \lambda tr(E)I + 2\mu E, \tag{2.24}$$

which is just Hooke's law from above with a different set of stress and strain tensors. The Saint Venant-Kirchhoff model is not a very relevant model for soft tissue mechanics, but its simplicity makes it convenient for illustrating general properties of the models, equations and solution process. It will be revisited in Chapter **??** to present finite element solvers for large-deformation solid mechancis.

2.4.2 Incompressible materials

A characteristic of soft tissues is that although they offer little resistance to deformations such as stretch or shear, they are very resistant against vol-

ume changes and are most correctly modeled as completely incompressible. This feature is shared with rubber-like materials, which is another important group of "soft" materials, and it gives rise to some additional challenges in formulating and solving mechanics models. Volume changes are quantified by the determinant of the deformation gradient, so a fully incompressible material satisfies $\det F = 1$ for all deformations. An important consequence of this condition is that the hydrostatic pressure in the material becomes completely decoupled from the deformation, a fact that may be illustrated by applying a uniform pressure to all sides of a cube made of an incompressible material. This will not give rise to any volume change, and therefore no deformation, but the applied pressure still has to be balanced by some internal stresses in the material. The strain tensor is zero while the stress is non-zero, which obviously does not fit with a stress-strain relation such as (2.24). Instead, to derive stress-strain relations for incompressible materials we may define the modified strain energy function

$$\Psi = \Psi(\mathbf{F}) - p(J-1), \tag{2.25}$$

which is defined only for $J = 1$, which is a constraint that must be enforced separately. At first sight this strain energy does not seem very useful, since the second term is always zero. However, this makes sense from a physical viewpoint since the hydrostatic pressure does not contribute to the strain energy in an incompressible material, just as no energy can be stored in an infinitely stiff spring. Furthermore, if we apply the formulas (2.22) and (2.22) to (2.22) we get

...

In order to derive strain energy formulationMore generally, the hydrostatic pressure in an incompressible material does not contribute to the strain energy and therefore cannot in general be determined from formulas like (2.22).

In practice, this condition is enforced in

As noted above, it is often convenient to formulate material laws in terms of the strain invariants rather than the strain tensor components directly. One simple example of an invariant-based material laws is the so-called neo-Hookean model, which is typically formulated as

$$\Psi(C) = C_1(I_{\mathbf{C}} - 3)$$

where C_1 is a material parameter and $I_{\mathbf{C}}$ is the first invariant of the right Cauchy-Green deformation tensor, i.e. $I_{\mathbf{C}} = tr(\mathbf{C})$. From (2.22) we have

$$\mathbf{S} = 2\frac{\partial \Psi}{\partial \mathbf{C}} = 2\frac{\partial \Psi}{\partial I_{\mathbf{C}}}\frac{\partial I_{\mathbf{C}}}{\partial \mathbf{C}} = \dots$$

TODO: Introduce the distinction between compressible and incompressible materials.

Chapter 3
Computational techniques for elasticity

Most of the continuum mechanics models derived in the previous section must be solved with numerical techniques. For the simplest models, typically linear elasticity and very simple geometries and loads, it may be possible to derive analytical solutions, and such solutions may be extremely valuable for verifying the accuracy of numerical solvers. However, large-deformation mechanics gives rise to non-linear equations that cannot be solved analytically, and to compute a solution the equations need to be discretized in space (and possibly in time), and the resulting non-linear algebraic equations must be solved with an iterative solution method. The standard numerical method for computational heart mechanics is the finite element method (FEM), which has a long tradition being the method of choice in solid mechanics, and is suitable for representing the complex and irregular geometry of the heart.

3.1 FEM for linear elasticity

A detailed discussion of the FEM is outside the scope of this book, and the interested reader is referred to one of many excellent introductions to the topic, for instance REFS. Here, we want to briefly introduce the method and show how it is applied to solve problems in heart mechanics. We start with the quasi-static formulation of the equation of motion, as derived in the previous chapter. Neglecting body forces and inertia, the problem can be written as

$$\nabla \cdot \sigma = 0 \text{ in } \Omega \tag{3.1}$$

$$\mathbf{u} = \mathbf{u}_0 \text{ on } \partial\Omega_d \tag{3.2}$$

$$\sigma \cdot n = T_0 \text{ on } \partial\Omega_s \tag{3.3}$$

Here we have used a combination of displacement and stress (load) boundary conditions. The foundation of the finite element method is the weak form of the PDE, which we obtain by multiplying (**??**) with a vector-valued test

function v and integrating over the domain Ω. In the mechanics community, this process is often given a physical interpretation, and is referred to as the *principle of virtual work*. The test function v is named a virtual displacement, which when multiplied with the stress gives rise a virtual work. The solution method proceeds to find the deformation state where this work vanishes for all virtual displacements ϕ. The typical text book in solid mechanics will never use the term *weak form*, and the notation and terminology is often quite different from other fields where the FEM is applied. Adding further to the potential for confusion is the fact that the FEM can also be derived as a minimization problem, where we find the deformation that minimizes the total (strain) energy of the elastic body. However, all of these derivations are completely equivalent and result in the same discretized equations, and in this book we will stick with the term weak form and the more "mathematical" tradition of the FEM field.

To derive the weak form of the linear elasticity problem, we multiply (3.1) with a vector-valued test function and integrate over Ω;

$$\int_{\Omega} (\nabla \cdot \sigma) \cdot v \, dx = 0,$$

which is to be satisfied for all test functions v. Applying Green's theorem, we get

$$\int_{\Omega} \sigma : \nabla v \, dx - \int_{\partial\Omega} v \cdot \sigma \cdot \mathbf{n} \, ds = 0,$$

and if we apply the boundary condition (3.2) and choose the space of test functions so that they vanish on Ω_d, we get

$$\int_{\Omega} \sigma : \nabla v \, dx - \int_{\partial\Omega} v \cdot T_0 \, ds = 0, \tag{3.4}$$

This form of the equation is quite general, and applies both to large- and small-deformation elasticity problems, regardless of which constitutive law is used. For this first example we consider linear elasticity, and insert the expression for the stress tensor in (**??**). The final weak form can then be summarized as: find $\mathbf{u} \in V$ such that:

$$a(u, v) = L(v) \forall v \in V, \tag{3.5}$$

with

$$a(u,v) = \int_\Omega \sigma(u) : \nabla v \, dx, \tag{3.6}$$

$$\sigma(u) = 2\mu\epsilon + \lambda(\nabla \cdot \mathbf{u})\mathbf{I} \tag{3.7}$$

$$L(v) = \int_{\partial\Omega} T \cdot v \, ds. \tag{3.8}$$

An alternative and more common form of (3.6), which arises from the symmetry of the stress tensor, is

$$a(u,v) = \int_\Omega \sigma(u) : \epsilon(v) \, dx,$$

with

$$\epsilon(v) = \frac{1}{2}(\nabla v + \nabla v^T).$$

The latter form arises naturally from minimization of the total elastic energy, and is closely linked with the Cauchy stress and the small-deformation strain tensor being a work-conjugate pair, as described in the previous chapter (REF).

To implement a traditional finite element solver based on (**??**), one would proceed to introduce a finite-dimensional subspace of $\hat{V} \subset V$, and approximate the solution $\mathbf{u}$ by a weighted sum of basis functions of $\hat{V}$; $\mathbf{u} \approx \sum_{i=1}^{n} c_i v_i$. The derivation can be found in multiple text books on the finite element method, and leads to a linear system of equations for the solution coefficients c_i. The implementations in this book are based on FEniCS, which automates a number of these steps. In the FEniCS code one will simply define appropriate function spaces for the solution and the test functions, input the weak form in a language close to the mathematics, and call on builtin FEniCS functionality for building and solving the system of linear equations. A complete FEniCS code for the linear elasticity problem looks as follows:

CODE BLOCK HERE

3.2 FEM for non-linear elasticity

Let us now turn to the more relevant non-linear elasticity problem. As noted above, the form (**??**) is quite general, and also applies in the large deformation case. However, this problem requires integrating over the deformed domain Ω, which for large-deformation problems is unknown. It is therefore more convenient to formulate the weak form relative to the undeformed configuration, using the appropriate stress and strain measures presented in the previous chapter. We have the equation of motion on the form

$$\int_{\Omega} (\nabla \cdot \mathbf{P}) \cdot v \, dx = 0.$$

Recall the important distinction that the ∇ operator in this case implies differentiation with respect to the reference (or material) coordinates, while in (3.1) we differentiated with respect to deformed (or spatial) coordinates. We proceed following the same steps as above, by multiplying with a vector test function v, integrating by parts (Green's theorem) and using the boundary conditions, to get

$$\int_{\Omega_0} \mathbf{P} : \nabla v \, dx - \int_{\partial\Omega_0} v \cdot T_0 \, ds = 0. \tag{3.9}$$

As above, we now insert the relevant stress-strain relation, typically defined in the form of a strain energy function. Using the neo-Hookean material as an example, we have

$$\mathbf{P} = \frac{\partial \Phi}{\partial \mathbf{F}},$$

with

$$\Phi = c_1(I_1 - 3), \quad I_1 = tr(E).$$

Although the formulation of the weak form looks the same as for the linear case above, the weak form in (3.9) is non-linear, and the subsequent finite element discretization leads to a set of non-linear algebraic equations. These equations need to be solved using Newton's method or a similar iterative technique, and the steps to linearize and solve equations of the form (3.9) is included in many text books on non-linear solid mechanics. Since we will again apply the FEniCS framework to solve the problem, the steps of linearizing and solving non-linear equations is automated as well as the finite element discretization process. As for the case of linear elasticity, it is sufficient to specify the necessary function spaces, formulate the appropriate weak form, and call on builtin FEniCS functions to discretize and solve the problem. The complete code looks for the simple neo-Hookean elastic solid looks like

CODE BLOCK HERE

- Put a "manual" linearization in an appendix
- Element choices, incompressibility and locking

3.2.1 Finite Element Formulations

The differential equation in (2.14) must be solved by applying a numerical method. For elasticity problems in general, and the non-linear heart mechanics problem in particular, the main method of choice has been the finite

element method. The finite element method is based on the weak form of (2.14), which can be established using a variational principle. One approach is to employ the principle of virtual work [**?**]. Alternatively, we can use the principle of minimum potential energy [**?**, **?**]. In this section we apply what is referred to as Galerkin's method [**?**], which is a formulation that is well suited when using the finite element method.

In the finite element method, the continuous displacement field $\mathbf{u}$ is approximated by a vector of nodal values $\mathbf{v}$ and a set of basis functions $\mathbf{N}$,

$$\mathbf{u} \approx \hat{\mathbf{u}} = \mathbf{N}\mathbf{v}.$$

The basis functions $\mathbf{N}$ depend on the reference coordinates $\mathbf{X}$. Furthermore, the derivatives of the continuous displacements may be approximated by

$$\frac{\partial \mathbf{u}}{\partial \mathbf{X}} \approx \frac{\partial \hat{\mathbf{u}}}{\partial \mathbf{X}} = \nabla^T \mathbf{N}\mathbf{v} = \mathbf{B}\mathbf{v}, \tag{3.10}$$

where $\mathbf{B} = \nabla^T \mathbf{N}$ is a matrix containing derivatives of the basis functions; $\frac{\partial N_i}{\partial X_j}$.

To establish the weak formulation in the matrix-vector notation, we generally multiply (2.14) by some test (or trial) functions, and integrate over the volume Ω of the continuum. In Galerkin's method the test functions are equal to the basis functions $\mathbf{N}$ for the displacement field. Hence, we obtain

$$\int_\Omega \mathbf{N}^T \nabla \left(\mathbf{F}\mathbf{S}\right) dV = \mathbf{0}.$$

Now, integrating by parts and employing (3.10), we end up with

$$\int_\Omega \mathbf{B}^T \mathbf{F}\mathbf{S} dV = \int_{\partial\Omega_\sigma} \mathbf{N}^T \mathbf{T} dS. \tag{3.11}$$

One observes that the natural boundary condition for the prescribed traction forces in (2.16) has been incorporated into the weak form of the equation.

Solving the Non-Linear Equations. For the problems of consideration, the weak form in (3.11) generally produces a system of non-linear equations to be solved for the unknown displacement field. Hence, iterative solution techniques are needed. We apply a common technique for solving non-linear equations, namely an incremental/iterative method of Newton's type, referred to as Newton-Raphson's method [**?**, **?**]. This technique requires a consistent linearization of all quantities, and results in efficient recurrence update formulas.

After linearizing and also including the discrete displacement field $\mathbf{v}$, we obtain a set of (linear) equations with $\Delta\mathbf{v}$ as unknowns. For each iteration we solve the linear system of equations, and update the discrete solution $\mathbf{v}^\ell$ by the solution $\Delta\mathbf{v}$,

$$\mathbf{v}^{\ell} = \mathbf{v}^{\ell-1} + \omega \Delta \mathbf{v},$$

where ℓ is the iteration number, and ω is a relaxation parameter. This iterative process is repeated until some convergence criterion is fulfilled.

Linearizing the Second Piola-Kirchhoff Stress Vector. JS 1: This section is to be removed or substantially rewritten. Most likely there is no need to present the matrix-vector notation. Employing the matrix-vector notation, an incremental decomposition of the second Piola-Kirchhoff stress vector in (xxx) may be written

$$\mathbf{S}^{\ell} = \mathbf{S}^{\ell-1} + \Delta \mathbf{S}, \tag{3.12}$$

where $\mathbf{S}^{\ell}$ is the unknown stress vector at iteration ℓ, $\mathbf{S}^{\ell-1}$ is the stress vector from the previous iteration, and $\Delta\mathbf{S}$ is the increment of the stress. The increment of the stress can be expressed in terms of the elasticity properties and the strains, as follows

$$\Delta \mathbf{S} = \mathbf{D} \Delta \mathbf{E}, \tag{3.13}$$

where $\Delta\mathbf{E}$ is the increment of the Green-Lagrange strain vector. Moreover, the matrix $\mathbf{D}$ contains components of the elasticity tensor $\mathcal{C}$, evaluated at iteration $\ell - 1$, yielding [**?**]

Linearization of the Governing Equation on Weak Form. In addition to linearizing the second Piola-Kirchhoff stress vector, we also need to linearize the remaining parts of the governing equation.

$$\int_{\Omega} \mathbf{B}^T \left[\left(\mathbf{H} + \frac{\partial \hat{\mathbf{u}}^{\ell-1}}{\partial \mathbf{X}}_F + \frac{\partial \boldsymbol{\Delta}\mathbf{u}}{\partial \mathbf{X}}_F \right) \left\{ \mathbf{S}^{\ell-1} + \mathbf{D} \left[\left(\mathbf{H}^T + \frac{\partial \hat{\mathbf{u}}^{\ell-1}}{\partial \mathbf{X}}_E \right) \frac{\partial^{\mathbf{v}} \boldsymbol{\Delta}\mathbf{u}}{\partial \mathbf{X}} + \frac{\partial \boldsymbol{\Delta}\mathbf{u}}{\partial \mathbf{X}}_E \frac{\partial^{\mathbf{v}} \hat{\mathbf{u}}^{\ell-1}}{\partial \mathbf{X}} \right] \right\} \right] dV = \int_{\partial\Omega_{\sigma}} \mathbf{N}^T \mathbf{T} dS. \tag{3.14}$$

Chapter 4
Constitutive laws for passive heart tissue

To limit the scope, and keep the focus on commonly used models, the focus should probably be on hyper-elasticity. Still, some justification of why we disregard visco-elastic effects should probably be included.

4.1 Modeling soft tissues

- Brief description of the exponential stress-strain behavior characteristic of soft tissues
- Simple constitutive laws based on strain components and strain invariants

4.2 Cardiac microstructure and anisotropy

(Possibly split this section in two, one covering standard anisotropic continuum models, and one focusing on the microstructure and related models.)

- Recapture and expand the description of cardiac microstructure from Chapter 1.1.2, and how this affects cardiac mechanical properties.
- Describe the necessary expansions of the models above to describe orthotropic and transversely isotropic material behavior, including examples of constitutive laws based on strain components and strain (pseudo-)invariants.
- Introduce the idea of a local (fiber) coordinate system, and how this enters the strain component based constitutive laws.
- Similar notes on spatially varying material directions for invariant-based models.

- Referring back to the first item above, introduce models that explicitly describe the cardiac microstructure, and discuss the fundamental differences from the continuum models.

4.3 Fitting material parameters

The purpose of this section is to give the readers a very brief introduction to how experiments are used to select the material parameters, and in particular to illustrate the difficulty and uncertainty associated with this part of the modeling.

- Brief review of experimental techniques to characterize passive material response, i.e. uniaxial and biaxial tests, shear tests etc. Not intended to be a complete presentation or discussion of experimental techniques, but discuss the different setups with respect to their ability to characterize anisotropic behavior.
- Brief review of material parameters encountered in the litterature, to illustrate variability
- Promises and limitations of image based techniques, for patient specific parameter fitting.

4.4 Computational techniques for passive muscle tissue

Present the necessary extensions of the solution methods from Chapter 3, in order to solve the equations of anisotropic hyeprelastic models with spatially varying material directions.

The equations derived above, (2.14)-(2.16) are completely general, in the sense that tehy apply to all kinds of materials. As long as the deformation satisfies the assumptions of negligible acceleration term and body force, it can be described by the equations above. Naturally, any deformation will be highly dependent not only on the forces acting on the material of study (which is included in the equations above), but also on the mechanical properties of the material involved. The material properties enter the equation above through so-called *constitutive laws*, which define a relation between the stresses and strains in a material.

The simplest possible stress-strain relation, which is applicable in a wide range of engineering materials and cases is known as Hookes law. It defines a linear relation between stress and strain in a material. In the simple case of uniaxial stretch, as illustrated in Figure xxx. Hookes law can be expressed as

$$\sigma = E\epsilon. \tag{4.1}$$

Here $\epsilon = \Delta L/L$ is a measure of strain, $\sigma = F/A$ is stress, and E is a material parameter known as Youngs modulus. In the more general case of 3D deformations, the corresponding relation is Hookes generalized law, given by

$$\sigma_{ij} = C_{ijkl}\epsilon_{kl}. \tag{4.2}$$

Since C_{ijkl} has four indices, each running from one to three, this tensor in general has 81 entries. However, because of known symmetry properties of this tensor it is possible to reduce this number to 21. Furthermore, for an isotropic material (the material properties are the same in all directions), Hookes generalized law can be simplified to depend on include only two independent parameters.

The example of Hookes law was merely included to provide a simplified example of a stress strain relation, to ease the understanding of more advanced constituitive laws. Hookes law assumes linear material behavior, and is also only applicable for small deformations, and none of these requirements apply to heart tissue. This necessitates far more complex constitutive laws in order to describe the material behavior of the muscle.

Biological tissues, including muscle tissue, is often modeled as *hyperelastic*. By assuming hyperelasticity, one is able to introduce a so-called strain energy potential function that defines a constitutive law for the material.

A hyperelastic material is path-independent when undergoing deformations. The work done by the stresses during a deformation process depends on the initial state and the final deformed state only. Hence, the deformation can be expressed by an *elastic potential* or a *stored strain energy function* per unit volume, Ψ. Moreover, the second Piola-Kirchhoff stress tensor is expressed as the derivative of Ψ with respect to the components of the Green-Lagrange strain tensor $\mathcal{E}$ [**?**, **?**],

$$\mathcal{S}(\mathcal{E}, \mathbf{X}) = \frac{\partial \Psi}{\partial \mathcal{E}} \tag{4.3}$$

Along with an expression for the path-independence, (4.3) is often used as the definition of a hyperelastic material [**?**].

The elastic properties of the material can be expressed by a fourth-order elasticity tensor $\mathcal{C}$ (not to be confused with $\mathbf{C}$ above), which depends on the deformation. It is defined as the derivative of the second Piola-Kirchhoff stress tensor with respect to the components of the Green-Lagrange strain tensor

$$\mathcal{C} = \frac{\partial \mathcal{S}}{\partial \mathcal{E}} = \frac{\partial \Psi}{\partial \mathcal{E} \partial \mathcal{E}} = 4\frac{\partial \Psi}{\partial \mathbf{C} \partial \mathbf{C}}.$$

This tensor is similar to the tensor introduced in Hookes generalized law above, in that it generally has 81 components that can be reduced to 21 because of symmetry. The tensor can be interpreted as an instantanous elasticity tensor for the material, which characterizes the stress strain relation in a small region around the current deformation state.

4.4.1 Constitutive Laws for Muscle Tissue

The material behavior of the heart muscle may be divided in two. First, we have the passive material behavior, which relates the force to the deformation in a relaxed muscle. Second, there is the active contractile force developed by the muscle. These two types of material behavior have typically been modeled quite separately both for skeletal muscle and heart muscle. The passive material properties are typically described as a non-linearly (hyper)elastic material, while the active contraction is modeled as an additional stress term which depends on the electrical activation state of teh muscle. In this section we give a short introduction to non-linearly elastic constitutive laws in general, and then describe som of the more influential models for heart muscle behavior, both passive and active.

(A more complete overview of cardiac tissue models in particular, may be found in, e.g., [**?**].)

4.4.1.1 The "Pole-Zero" Cardiac Tissue Model

A well established material model for cardiac tissue is the so-called "pole-zero" model, see, e.g., [**?**]. The strain energy function is given by

$$\begin{aligned}\Psi = k_{ff}\frac{\mathcal{E}_{ff}^2}{|a_{ff}-\mathcal{E}_{ff}|^{b_{ff}}} + k_{ss}\frac{\mathcal{E}_{ss}^2}{|a_{ss}-\mathcal{E}_{ss}|^{b_{ss}}} + k_{nn}\frac{\mathcal{E}_{nn}^2}{|a_{nn}-\mathcal{E}_{nn}|^{b_{nn}}} \\ + k_{fs}\frac{\mathcal{E}_{fs}^2}{|a_{fs}-\mathcal{E}_{fs}|^{b_{fs}}} + k_{fn}\frac{\mathcal{E}_{fn}^2}{|a_{fn}-\mathcal{E}_{fn}|^{b_{fn}}} + k_{sn}\frac{\mathcal{E}_{sn}^2}{|a_{sn}-\mathcal{E}_{sn}|^{b_{sn}}}.\end{aligned}$$

Here, $\mathcal{E}_{ij}$ are components of the Green-Lagrange strain tensor referred to the local fiber direction (f), the fiber sheet direction (s), which is normal to the fiber direction, and the fiber normal direction (n). Moreover, k_{ij}, a_{ij}, and b_{ij} are constitutive parameters referred to the local fiber coordinate system. The values of a_{ij} denotes the limiting strains, or poles. An underlying assumption of this model is that the material has an orthotropic behavior.

4.4.1.2 An Exponential Cardiac Tissue Model

A set of alternative constitutive laws for the cardiac tissue are expressed as exponential functions. As an example, we consider a non-linear, transversely isotropic, hyperelastic model, which for an almost incompressible material may be written [**?**],

$$\Psi = \frac{1}{2}K(e^W - 1) + C_{compr}(J \ln J - J + 1), \tag{4.4}$$

where

$$W = b_{ff}\mathcal{E}_{ff}^2 + b_{xx}(\mathcal{E}_{nn}^2 + \mathcal{E}_{ss}^2 + \mathcal{E}_{sn}^2 + \mathcal{E}_{ns}^2) + b_{fx}(\mathcal{E}_{fn}^2 + \mathcal{E}_{nf}^2 + \mathcal{E}_{fs}^2 + \mathcal{E}_{sf}^2). \tag{4.5}$$

As for the pole-zero law, $\mathcal{E}_{ij}$ are the components of the Green-Lagrange strain tensor referred to the local fiber (f), fiber sheet (s), and fiber normal (n) axes. Furthermore, K, b_{ff}, b_{fx}, and b_{xx} are material parameters, J is the determinant of the deformation gradient, and C_{compr} represents the empirically observed bulk modulus. The material parameters in (4.4) and (4.5) are typically determined from physical experiments.

The strain energy function in (4.4) can easily be extended to an orthotropic model. In that case (4.5) is replaced by

$$W = b_{ff}\mathcal{E}_{ff}^2 + b_{ss}\mathcal{E}_{ss}^2 + b_{nn}\mathcal{E}_{nn}^2 + b_{fs}(\mathcal{E}_{fs}^2 + \mathcal{E}_{sf}^2) + b_{fn}(\mathcal{E}_{fn}^2 + \mathcal{E}_{nf}^2) + b_{ns}(\mathcal{E}_{ns}^2 + \mathcal{E}_{sn}^2),$$

where b_{ff}, b_{ss}, b_{nn}, b_{fs}, b_{fn}, and b_{ns} are material parameters, and $\mathcal{E}_{ij}$ are the components of the Green-Lagrange strain tensor, as before. The above models have been used for several applications, see, e.g., [**?**, **?**], and the transversely isotropic version has been applied as a starting point for deriving a suitable strain energy function to be applied in the mixed formulation briefly presented in this report. Details are found in [**?**].

Chapter 5
Modeling cell and tissue contraction

In terms of limiting the scope, this may be the most difficult chapter. Clearly, covering all aspects of cell mechano-biology is not possible. My first thoughts are to ignore all electrophysiology, and carefully outline the scope and limitations at the start of the chapter. Then something like this:

5.1 Cardiomyocyte force development

- Expand on the general introduction given in Chapter 1 , to give a more detailed desription of how myocytes develop force.
- Describe important features that should be captured by a realistic model, including the cooperativity of the force-Ca relation, and the force-length and force-velocity relations. Focus on biophysical details and modelign issues, and briefly mention computational and numerical difficulties arising from these aspects.
- Present a model for force-development based on a cross bridge distortion model, in a relatively simple form, and illustrate how the model captures the features listed above.
- Possibly include a phenomenological model, i.e. based on the ideas introduced by the HMT model, as a model of substantially simplified computational complexity.

5.2 Cell to tissue coupling

- Describe coupling of single cell contraction to tissue mechanics, in terms of the standard active stress approach

- Possibly mention the active strain and hybrid approaches as alternatives to the standard form.
- Comment on computational and biophysical aspects of the two approaches

5.3 Computational models of active mechanics

- Expand the computational models introduced in Chapter **??**, to include the actively contracting muscle.
- Illustrate the challenges of strongly coupled simulations, and discuss suitable computational techniques.

During the heart beat an electrical pulse propagates through the heart wall, and the excitation of the muscle cells will in turn trigger the contraction of the muscle. The development of stresses due to the electrical activity is referred to as *active stresses*. When modeling the mechanical behavior of the heart, the second Piola-Kirchhoff stress tensor is typically written as the sum of a passive and an active part,

$$\mathcal{S} = \mathcal{S}^p + \mathcal{S}^a.$$

The passive stress $\mathcal{S}^p$ is related to the mechanical behavior of the cardiac tissue itself, and has been dealt with in previous sections of this report. Now, we consider the active stress tensor $\mathcal{S}^a$.

The active Cauchy stress tensor, referred to local fiber coordinates, is commonly expressed as [**?**]

$$\sigma^a = \begin{pmatrix} \sigma^a_{ff} & 0 & 0 \\ 0 & \sigma^a_{ss} & 0 \\ 0 & 0 & \sigma^a_{nn} \end{pmatrix}, \tag{5.1}$$

where σ^a_{ff}, σ^a_{ss}, and σ^a_{nn} are the active normal stresses in the fiber (f), the fiber sheet (s), and the fiber sheet normal (n) directions, respectively. The active shear stresses are assumed to be zero. Furthermore, the local active Cauchy stress tensor is related to the local active second Piola-Kirchhoff stress tensor through

$$\mathcal{S}^a = J\mathcal{F}^{-1}\sigma^a\mathcal{F}^{-T}.$$

Local contributions are expressed in global coordinates using transformation matrices, see Section xxx.

Because of the lack of suitable experimental models for estimating the transverse active normal stresses in (5.1), a frequently applied simplification is setting these components equal to zero. In this way the only non-zero component in the active Cauchy stress tensor is the fiber normal stress σ^a_{ff}.

However, Lin and Yin [?] showed that the forces generated in the transverse directions are in the range of 20-60% of active fiber tension in rabbit myocardium. Also, in recent studies the transverse active stress components σ^a_{ss} and σ^a_{nn} have been included as a function of σ^a_{ff} and local transverse and axial strains, to be consistent with biaxial experimental tests [?, ?, ?]. Hence, the modeling for the actively contracting myocardium should contain contributions from all (local) diagonal components.

Several active fiber normal stress models of different complexity have been developed over the years, see, e.g., [?, ?, ?] and references therein. In this report we give two examples; a simple linear model [?], and the advanced Hunter-McCulloch-terKeurs (HMT) model [?].

The HMT Model. According to Sachse [?] the HMT model is one of the most advanced models for active force development. The HMT model includes i) the intracellular calcium concentration Ca, ii) the rapid binding of Ca to troponin C and its slower tension-dependent release, iii) the kinetics of tropomyosin movement and availability of cross-bridge binding sites, and the length-dependence of this process, and iv) the kinetics of cross-bridge tension development under perturbations of myofilament length. In the following, we describe the main parts of the HMT model.

The intracellular calcium concentration is contained in models for describing muscle cell electrophysiology, such as the Beeler-Reuter model [?], the Luo-Rudy model [?] and the model by Winslow et al. [?]. In these cell models the uptake to and from the sarcoplasmic reticulum (SR), which is an important contribution to the total amount of Ca, is taken into account. The intracellular calcium concentration may alternatively be established from experiments, and a convenient representation of the time-dependent intracellular Ca twitch transient is [?]

$$Ca_i(t) = Ca_o + (Ca_{max} - Ca_o)\frac{t}{\tau_{Ca}} e^{1-t/\tau_{Ca}},$$

where $Ca_i(t)$ is the concentration of Ca. The resting level is denoted Ca_o, and the maximum value Ca_{max} is achieved at time $t = \tau_{Ca}$. This time-dependent function for the intracellular calcium concentration is close to the measurements obtained by Stuyvers et al. [?] for rat trabeculae. Note that the concentration of intracellular calcium in this model does not vary in space.

The binding and release of Ca to troponin C (TnC) is very fast, and it is believed to be limited by diffusion gradients from the junctional SR release site to the TnC binding site. It also depends on the mechanical state of the muscle. An isotonic twitch terminates much quicker than an isometric twitch, and if the muscle is subjected to a quick release during the twitch, the ability to generate forces is reduced rapidly. These latter phenomena are explained by the release of Ca from TnC. The release and binding of Ca to TnC has been studied for both skeletal and cardiac muscles [?,?,?,?,?,?,?]. To model the Ca-TnC binding kinetics, the following equation is proposed [?],

$$\frac{dCa_b}{dt} = \varrho_0 Ca_i(Ca_{bmax} - Ca_b) - \varrho_1 \left(1 - \frac{\sigma^a_{ff}}{\vartheta \sigma^a_o}\right) Ca_b, \tag{5.2}$$

where Ca_i is the concentration of free myoplasmic Ca, and Ca_b is the concentration of Ca bound to the calcium specific binding site on TnC. Moreover, Ca_{bmax} is the maximum value of Ca_b attained at equilibrium when $\sigma^a_{ff} = \vartheta \sigma^a_o$, where ϑ is a scalar parameter value, and σ^a_o is the isometric fiber normal stress. Attachment is governed by the rate constant ϱ_0, and detachment at zero active stress is governed by the rate constant ϱ_1. Parameter values for the quantities in (5.2) are estimated from experiments by Hofman and Fuchs [**?**, **?**].

The binding of Ca to TnC initiates changes of the configuration of the thin filaments. This allows cross-bridges to be formed between the thin and thick filaments, i.e. the myosin head binding to the actin, resulting in development of forces [**?**, **?**]. The tropomyosin kinetics is modeled by [**?**]

$$\frac{dz}{dt} = \alpha_0 \left[\left(\frac{Ca_b}{C_{50}} \right)^n (1 - z) - z \right]. \tag{5.3}$$

Here, z is a non-dimensional parameter ($0 \leq z \leq 1$) representing the proportion of actin sites available for cross-bridge binding. Moreover, α_0 is the rate constant of "tropomyosin movement", and C_{50} and n are the Hill parameters [**?**].

Under steady state conditions the proportion of actin sites available for cross-bridge binding is found by requiring that $dz/dt = 0$ in (5.3). This results in the relation

$$z_{SS} = \frac{(Ca_b)^n}{(Ca_b)^n + (C_{50})^n}. \tag{5.4}$$

Hofman and Fuchs [**?**, **?**] reported direct evidence that length-dependent effects on Ca binding to TnC are mediated via cross-bridge attachments. Under isometric conditions the tension-length relation may be shown to be dependent of calcium through the algebraic relation [**?**]

$$\sigma^a_o(\lambda, z) = \sigma^a_{ref}(1 + \beta_0(\lambda - 1))z,$$

where z is obtained from solving (5.3), or, in case of a steady state situation, from (5.4). Moreover, σ^a_{ref} is the reference stress at $\lambda = 1.0$, whereas $\beta_0 = 1/\sigma^a_{ref} \cdot d\sigma^a_o/d\lambda$.

Experiments done by Kentish et al. [**?**] clearly indicate that the Hill parameters in (5.3) (and (5.4)) must be length-dependent. Hunter et al. [**?**] found that a linear length-dependence is sufficient to model the full range of the isometric active stresses, i.e.

$$n = n_{ref}(1 + \beta_1(\lambda - 1))$$

and

$$pC_{50} = pC_{50ref}(1+\beta_2(\lambda-1)),$$

such that

$$C_{50} = 10^{6-pC_{50}}.$$

The parameter values of the constants σ^a_{ref}, β_0, n_{ref}, β_1, pC_{50ref} and β_2 are determined by fitting the model results to experimental data obtained by Kentish et al. [**?**] for skinned rat trabeculae. However, some of the values are anomalously high [**?**]. The set of parameter values are therefore slightly modified.

To complete the model, we analyze cross-bridge kinetics, which is modeled by the so-called *fading memory model* [**?**, **?**]. Applying this model, the active fiber stress may be written as [**?**]

$$\sigma^a_{ff}(t) = \sigma^a_o \frac{1+aZ}{1-Z}. \tag{5.5}$$

In the above expression a is a constant value. Moreover, the model includes a non-linear function $Z(\sigma^a, \sigma^a_o)$. It can be argued that the following non-linear function Z can be chosen

$$Z(\sigma^a, \sigma^a_o) = \sum_{i=1}^{3} A_i \int_{-\infty}^{t} e^{-\alpha_i(t-\tau)} \mathring{\lambda}(\tau) d\tau, \tag{5.6}$$

where $\mathring{\lambda} \equiv d\lambda/dt$, and A_i and α_i $(i = 1,2,3)$ are parameters determined from experiments [**?**]. A small time step Δt is assumed to produce a small change in λ. Hence, for each time step, $\mathring{\lambda}_k = \frac{\Delta\lambda_k}{\Delta t_k}$ is assumed to be constant, where $\Delta\lambda_k = \lambda(t-\Delta t) - \lambda(t-2\Delta t)$, i.e. the stretch values at the two previous time steps. The total integral in (5.6) may then be written as the sum

$$Z = Z^0 + Z^1 + Z^2 + ... + Z^k,$$

where k is the time step number, and

$$Z^k = \frac{\Delta\lambda_k}{\Delta t_k} \sum_{i=1}^{3} A_i \int_{t-\Delta t_k}^{t} e^{-\alpha_i(t-\tau)} d\tau = \frac{\Delta\lambda_k}{\Delta t_k} \sum_{i=1}^{3} \frac{A_i}{\alpha_i} \left(1 - e^{-\alpha_i \Delta t_k}\right). \tag{5.7}$$

In the above expression we have taken into account the possibility of adaptive (or non-constant) time stepping. For the hereditary integral we also assume that the contribution for $t < 0$ is negligible compared to that from $t \geq 0$. This may be justified by assuming that the change in sarcomere length $\Delta\lambda$ is close, or equal, to zero prior to $t = 0$, and by the fading memory assumption.

Figure xxx displays the active normal fiber stress in (5.5) as a function of time for different fiber stretch values λ. Panel xxx of Figure xxx shows the

dynamic state, whereas panel xxx displays the steady state situation. The λ value is held constant in time.

Chapter 6
Boundary conditions and whole heart models

Chapter 7
Boundary conditions and whole heart models (20-30 p)

In the interest of saving space, this should probably not cover whole heart models, but rather a simplified LV model. This choice will allow the description of most of the general features and challenges of whole heart models, without including too much detail. Possible contents will include:

7.1 The cardiac cycle revisited

- Recapture the phases of the cardiac cycle introduced in Chapter 1, and describe how these are connected to valvular events and the mechanics of the circulatory system.
- Introduce the concept of ventricular BCs by considering passive filling with a prescribed pressure

7.2 Models for the circulatory system

- Introduce a simple closed loop model for the hemodynamic boundary conditions,
- Comment on limitations and possible extensions of the simple model, but refer to other sources for actual models

7.3 Computational models of the beating heart

- Comment on implications for solution methods, and present extensions of previously derived methods to describe the full dynamic problem

- Examples of interesting simulation cases
- Possible discussion of limitations and possible extensions
- Biventricular models, either discussed as a possible extension or included in the form of a simple example

Chapter 8
Open problems in cardiac mechanics

Chapter 9
Open problems in cardiac mechanics

Describe open problems and unsolved challenges in cardiac mechanics modeling. This is still fairly open, but possible candidate sections include:

- The clinical perspective. What are the unsolved clinical challenges where (improved) mechanics models are promising tools?
- Understanding myocyte contraction, and the multiscale aspects of this process. While the microscopic scale of cell contraction may be well understood, there are unresolved questions in how the microscopic behavior can be properly incorporated into organ-scale models.
- Variability of material properties. Even for passive mechanics, the variability in reported material properties and parameters does not inspire confidence in model predictions. Should be discussed in view of the current modeling paradigm and the in vitro and in vivo techniques used for parameter fitting.

Remark. Documents that contain raw Mako code in verbatim code blocks cannot also be processed by Mako, and this is the case with the `mako` chapter. Since we need Mako for processing the rest of this book document, we are forced to compile the `mako` chapter as a stand-alone document (with the `--no_mako` option) and let this appendix be just a link to the this stand-alone document[1].

[1] `http://hplgit.github.io/setup4book-doconce/doc/pub/mako/pdf/main_mako.pdf`